	Proc. XIVth Int. Congr. on Rheology *Edited by:*	August 22-27, 2004 Seoul, Korea

Recent Developments in Shear and Extensional Microrheometry of Complex Fluids

Gareth H. McKinley

Hatsopoulos Microfluids Laboratory
Department of Mechanical Engineering, M.I.T., Cambridge MA 02139, USA

ABSTRACT

We review the design and construction of several new microrheometers designed to facilitate the study of non-Newtonian fluids using very small sample volumes (1-10 μl) and on length scales of micrometer dimensions. These devices enable both the steady shear and transient extensional rheological properties of complex fluids to be measured. The shear-rate-dependent viscosity and gap-dependent yield stress of a fluid sample are measured using a sliding plate microrheometer with optical flats as the shearing surfaces. Compound flexure arrangements serve to generate a steady or oscillatory plane Couette flow and as the 'pick-up' or force transducer. Alignment fidelity, device orthogonality and total error stack-up are all optimized by machining the entire instrument frame from a single monolithic aluminum block using water-jet and EDM technology. The transient extensional rheology of very small samples is also measured using 1–100 μL fluid droplets in a microscale capillary break-up extensional rheometer. In this device, the extensional flow is driven by capillarity and resisted by the viscous and elastic stresses in the elongating fluid thread. These two devices are used to quantify the rheological properties of a wide range of complex fluids from consumer products to biopolymer solutions. Examples considered include mayonnaise and yogurt, biopolymer solutions such as the spinning dope extracted *ex vivo* from the silk worm, *Bombyx mori* and from the major ampullate gland of the *Nephila clavipes* spider, plus the physically-crosslinked mucin gel of slugs and snails.

INTRODUCTION

An electronic search of any bibliographic database will show that the usage of the terms microrheology and microrheometry has exploded over the past decade, and in particular in the years since the last International Congress. Advances in manufacturing capabilities, nanopositioning, and electro-optical diagnostics have combined to enable the design and construction of numerous devices capable of making microrheological measurements. In this plenary paper we review some of the experimental techniques and consider the ways in which they can be employed in the study of non-Newtonian materials.

Microrheometry may be defined conveniently as the *quantitative* measurement of the material functions of a complex fluid when one of the characteristic dimensions of the sample is on the micron scale. At such scales, the roughness of the test fixture surfaces, the gap separation and the characteristic length scale of the fluid microstructure may all interact. A wide variety of different techniques fall within the purview of microrheometry. These may be loosely subdivided into the classes shown in Figure 1. Space precludes a detailed review of each of these classes of instrumentation however further discussion may be found in several recent texts [1,2].

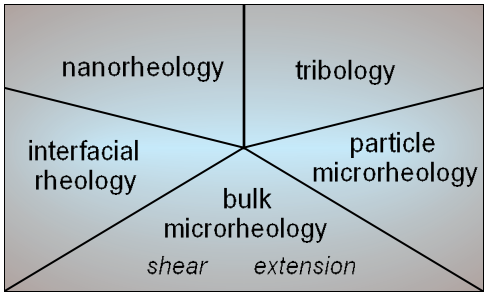

Figure 1. An overview of some of the different classes of microrheometric hardware.

The earliest microrheological studies involved the use of either passive (thermally-driven) or active (magnetically-or optically-translated) microbeads dispersed within the sample of interest [3]. Such techniques rely on correlative techniques or microscopic observation of the time-fluctuating displacement of the microbead(s) [4] and are very convenient for *in situ* observation of biological samples such as actin gels and for high-throughput screening [5].

At present they are inherently limited to measurements of the *linear* viscoelastic properties of the suspending matrix because of the need to invert a generalized Stokes-Einstein relationship connecting the measured displacement and the desired material function (a complex modulus or viscosity). More detailed reviews are given in [6,7].

In the present work we focus primarily on the adaptation of conventional 'bulk' or macro-scale rheological techniques involving boundary driven deformations (e.g. steady shear flow, uniaxial extensional flow). The benefits of such an approach include the ability to learn from existing instrumentation (such as conventional rheometers, the surface forces apparatus (SFA) and the atomic force microscope (AFM)), and the ability to measure nonlinear rheological properties under large strains and deformation rates. The gap separations and thread radii in the present study are typically kept to above 1 μm. As the gap separation decreases still further (say below 0.1 μm), long-range molecular interactions between the surfaces and the fluid become important and asperity contact leads to tribological characteristics in the fluid response. Recent developments in this emerging area of *nanorheology* are reviewed in [8].

SHEARING MICRORHEOMETRY

We first consider measurements of the steady shear viscosity of complex fluids. A Flexure-based Micro-Rheometer (FMR) has been developed that uses two optical flats (flat to within $\lambda/20 \approx 30$nm) as the shear surfaces. The FMR generates a plane Couette flow using a compound flexure design that is machined via water-jet and wire-EDM technology. The basic configuration of the instrument is shown in Figure 2.

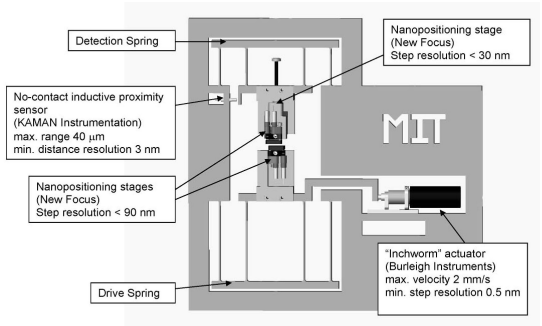

Figure 2. The flexure-based Microrheometer (FMR) and some of its design specifications

White light interferometry and a three-point nanopositioning stage employing piezo-stepping motors are used to control the parallelism of the upper and lower surfaces. The lower plate is attached to a drive flexure which is moved by an 'inchworm' motor with a resolution of 0.1 nm. Further details of the instrumentation are provided elsewhere (see ICR Poster #212 and [9]).

The instrument is able to impose steady or oscillatory stresses over a wide dynamic range (depending on the surface area of the optical flats) and shear rates from $0.01 \le \dot{\gamma} \le 100\text{s}^{-1}$. Optical access to the sample is also provided through the glass semi-silvered flats serving as the upper and lower plates. The device has been used to systematically probe the gap-dependent microrheology of microstructured foods such as mayonnaise and polymer solutions such as Xanthan gum [9].

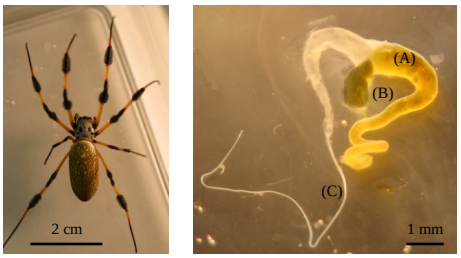

a **b**

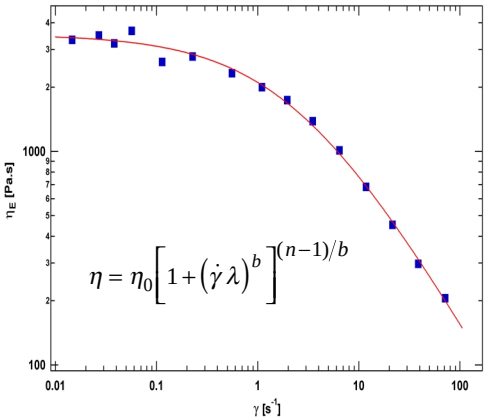

Figure 3. Steady shear viscosity of 1 μl droplet of silk dope from the major apullate gland of N.clavipes *(a,b); The Carreau-Yasuda parameters are; η_0= 3530 Pa.s; b = 0.68; n = 0.18; λ = 0.40s.*

The FMR is also of use in examining the viscometric properties of biopolymer solutions when it is only possible to harvest small volumes of fluid. An example of this latter application is the ex-vivo measurement of native silk spinning dopes obtained from the silkworm (*Bombyx mori*)

and the golden-orb weaving spider (*Nephila clavipes)*. Dissection of the major ampullate gland of *N. clavipes* (shown above in Figure 3(a)-(b)) typically yields less than 5 µl of a viscous birefringent liquid (labeled 'B'), consisting of a 35-40% concentrated solution of Spidroin protein [10]. In previous studies of silk rheology it has been necessary to dilute the silk liquor in order to measure the fluid rheology [11]. However, it is possible to use the FMR to provide a direct measurement of the shear viscosity of the native silk dope as shown in Figure 3(c). The material is a highly viscous liquid ($\eta_0 \geq 3500$ Pa.s) and is highly shear-thinning with a power law exponent $n \approx 0.18$ which is a hallmark of the liquid crystalline behavior of the silk solution [10]. The fluid rheology is well-fitted by the Carreau-Yasuda equation as shown in Figure 3(c) with a characteristic time constant $\lambda_c \approx 0.40$ s.

A second example is provided by the mucal films deposited by slugs and snails during locomotion. Bulk creep measurements have shown that these materials exhibit a yield stress and development of a time- and stress-dependent elastic gel-like structure [13, 14]. Structurally-sensitive gels can be probed in the FMR by imposing large amplitude oscillatory shearing (LAOS) deformations. The resulting stress-strain curves for a 40µm film of pedal mucus from *Limax maximus* are shown in Figure 4.

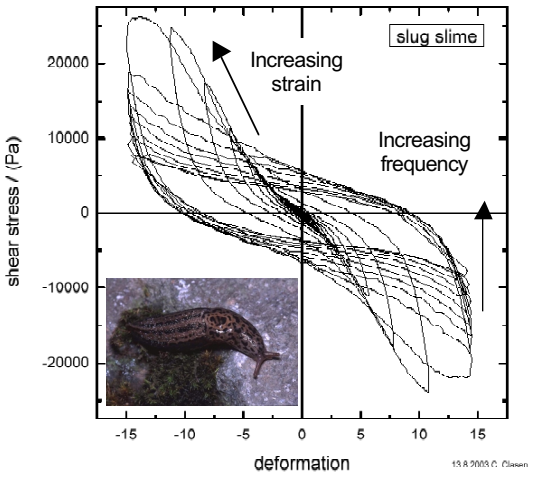

Figure 4. LAOS measurements and hysteresis in a 40µm film of pedal mucus from L. maximus

As the strain-amplitude is increased, the film shows a nonlinear elastic response characteristic of a strain-hardening viscoelastic network. At deformations close to a strain amplitude of $\gamma \approx 15$, the material softens and the hysteresis increases (characteristic of a nonlinear physically-crosslinked 'physical gel'). Increasing the frequency of oscillation further decreases the magnitude of the shear stress (because the material has less time to 'rebuild' the network structure) and increases the dissipative or fluid-like response. Understanding and emulating such a rheological response is important in developing synthetic mucus films for robotic limacine locomotion.

EXTENSIONAL MICRO-RHEOMETRY

The technique of capillary thinning and break-up has become a well-accepted technique for measuring the transient extensional rheology of liquid filaments [15-17]. An initially stable liquid bridge is axially deformed to generate a slender liquid filament which then undergoes necking under the action of capillary pressure. Viscous and elastic stresses in the thinning thread resist this necking motion. By monitoring the midpoint radius $R_{mid}(t)$ of the thread using a laser micrometer, or by analyzing axial profiles $R(z,t)$ of the fluid thread, it is possible to extract the characteristic time constant of an elastic fluid, or the viscosity of a Newtonian fluid [18]. Independent of choice of fluid model, it is also possible to define an 'apparent extensional viscosity' from the ratio of the capillary pressure in the filament and the instantaneous strain rate:

$$\eta_E(t) \cong \frac{\sigma}{-2\,dR_{mid}/dt}. \qquad (1)$$

where σ is the surface tension. The corresponding Hencky strain is given by integration of the strain rate:

$$\varepsilon = \int_0^t \dot{\varepsilon}(t')\,dt' = 2\ln\left(R_0/R(t)\right). \quad (2)$$

When very small sample volumes are available (such is in the case of native silk dopes) it is necessary to optimize the design of such capillary-thinning devices by using very small (~ 1mm) diameter endplates and tightly-focused laser micrometers. In this way it is possible to use a miniaturized capillary break-up extensional rheometer (or *µCABER)* to measure the transient extensional response of silk in an *ex-vivo* fashion, as shown in Figure 5.

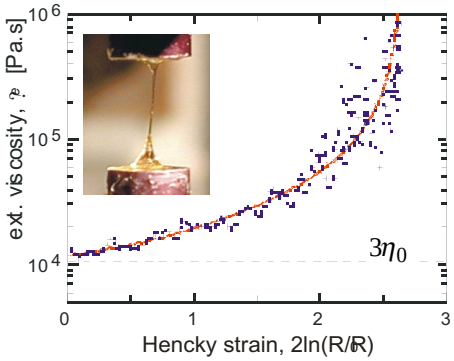

Figure 5 The transient extensional rheology of a droplet of spider silk (harvested from N. clavipes*) in a µCaber. Here R(t) is the radius of the thread at the midpoint between the plates. Inset, a silk thread of diameter 60 µm formed by separating the plates to a distance of 5 mm and allowing the thread to neck under the action of capillarity and viscoelastic stresses.*

The silk solution initially has an extensional viscosity that is close to three times the shear viscosity measured using the flexure-based microrheometer (cf. Figure 3); however the viscosity steadily climbs as a result of mass transfer and the drying of the thread. (The noise arises from the differentiation of the experimental midpoint diameter data). Eventually the filament solidifies with a diameter $D_\infty \approx 40$ µm (as shown in the inset) and the extensional viscosity diverges. If a constant tension is applied to the filament during the necking process (as in natural dragline spinning) then finer filaments result.

The use of capillary thinning and break-up experiments to characterize the extensional rheology of complex fluids used in industrial processes is particularly relevant when the process itself involves drop break-up or filament formation. Even though the kinematics are inhomogeneous, the filament thinning and necking process is closely related to the actual process of interest.

These capillary-thinning and/or break-up processes are governed by (at least) three characteristic time scales; the viscous time $t_v \sim \eta_0 R/\sigma$, the polymeric timescale λ and an inertial or Rayleigh time-scale $t_R \sim \sqrt{\rho R^3/\sigma}$ [19]. The relative balances of these time-scales (and the associated contributions to the total force in the fluid thread) can thus be represented in terms of two dimensionless parameters;

$$\text{Ohnesorge Number; } Oh = \frac{t_v}{t_R} \sim \frac{\eta_0}{\sqrt{\rho\sigma R}} \qquad (3)$$

$$\text{Deborah Number; } De = \frac{\lambda}{t_R} = \frac{\lambda}{\sqrt{\rho R^3/\sigma}} \qquad (4)$$

These two dimensionless parameters can be used to define a two-dimensional 'operating space' for instruments such as capillary break-up rheometers and other non-Newtonian free surface processes. Such a diagram is sketched in Figure 6 below.

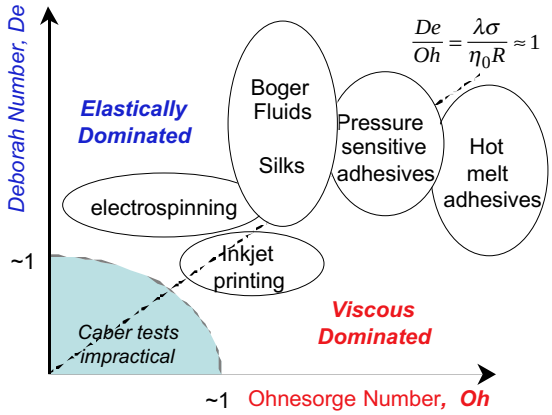

Figure 6 An 'operating diagram' for capillary-thinning and break-up flows of complex fluids; organized in terms of the natural time scales for capillary, viscous, and elastic phenomena.

For viscous fluids, the inertial time-scale t_R becomes unimportant and the dynamics of the thinning process depends on the relative magnitude of the viscous and elastic time scales; also known as the elasto-capillary number

$$E_s = \frac{De}{Oh} = \frac{\lambda}{t_v} = \frac{\lambda\sigma}{\eta_0 R}. \qquad (5)$$

Elastically-dominated and viscously-dominated necking processes are thus demarcated by the line $E \approx 1$ sketched in Figure 6.

However, in 'low viscosity' and 'weakly elastic' fluids, inertial effects often overwhelm the non-Newtonian stresses in the fluid making the extensional rheology difficult to measure (see e.g. [21]). A consideration of equations (3)-(4) above shows that as the length scale R decreases into the micrometer diameter, inertial forces in a fluid thread become progressively less important and viscoelastic forces once again dominate. Capillary-thinning instruments thus make excellent micro-extensional rheometers for 'low

viscosity non-Newtonian fluids' such as agricultural fertilizers, and inks or paints used in spraying operations.

For example; in operations such as electrospinning it is essential to be able to form a uniform filament in the absence of beads-on-a-string morphology; hence one requires $De \geq Oh > 1$; conversely in inkjet printing neither long elastic tails nor inertially-induced satellite drops are desirable; consequently one requires $De \approx Oh \approx 1$.

Capillary break-up tests become impractical when either $De \leq 1$ or $Oh \leq 1$ because inertial effects dominate the process resulting in strong asymmetries in the deformed fluid column and the formation of satellite droplets. The precise form of this lower boundary of operability however is also dependent on careful selection of geometric parameters such as the initial sample volume and the total stretch imposed on the filament. In order to investigate the limiting capabilities of such extensional microrheometers, we have performed detailed studies of dilute aqueous solutions of high molecular weight polymers such as polyethylene oxide using high speed digital videoimaging of the break-up process [19]. Two representative examples of the dynamical processes that evolve during the filament thinning and break-up process are shown in Figure 7 below.

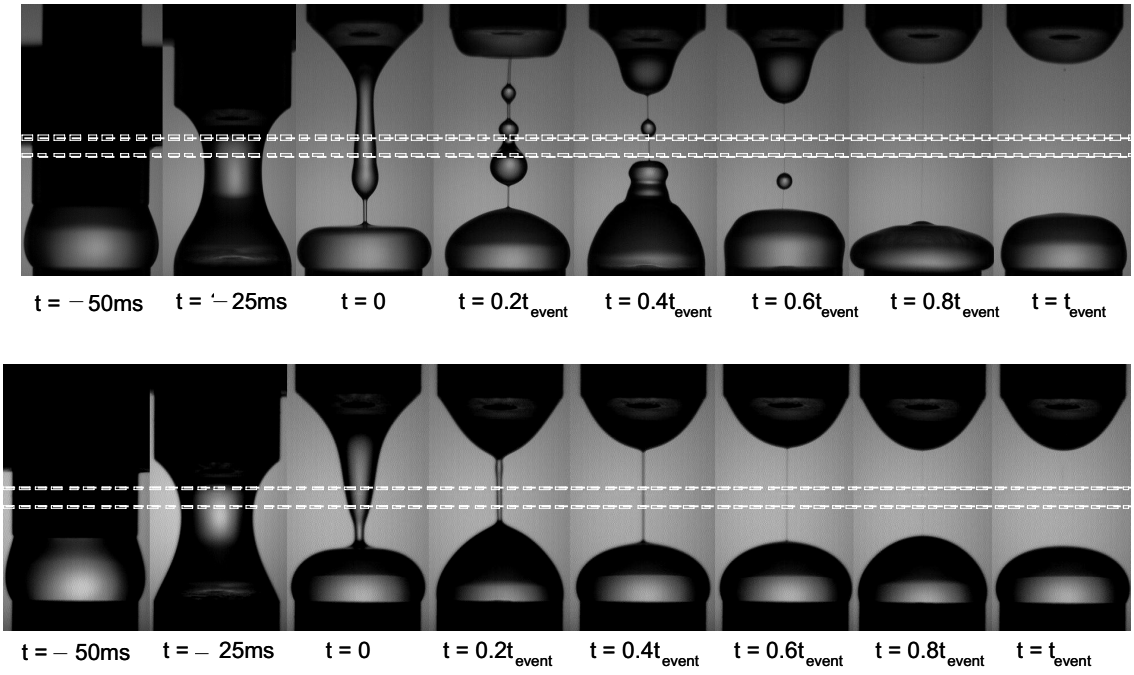

Figure 7. A sequence of high-speed digital video images showing the capillary-thinning and break-up of a 'low-viscosity' elastic fluid (in this case 0.1 wt% PEO, M_W = 2×10^6 g/mol). The upper sequence shows an imposed axial stretch over 50 ms to a final aspect ratio of $\Lambda_f = h_f / 2R_0 = 2$; the lower sequence shows a stretch of equal duration to a final aspect ratio of $\Lambda_f = h_f / 2R_0 = 1.6$. The plate diameter in each case is $2R_0$ = 6 mm and the fluid volume is ≈110μl. The broken lines show the location and beam-width of the laser micrometer which measures $D_{mid}(t)$.In each case the total break-up time is $t_{event} \approx$ 50ms.

When the final aspect ratio of the separation is too high (corresponding here to $\Lambda_f = h_f / 2R_0 \geq 1.8$) the low-viscosity fluid filament evolves into the well-known beads-on-a-string morphology. The sequence of images show that the beads may travel along the string and coalesce [23]. Elastic effects arising from molecular extension still dominate in the narrow thread-like regions however the presence of the large beads (in which surface tension dominates) disrupts the measurement. However, by decreasing the total imposed stretch, an axially uniform fluid thread is successfully obtained. Measurements of the radial evolution in the thread midpoint diameter then lead to measurement of a characteristic polymer relaxation time of $\lambda \approx 1.4 \pm 0.4$ ms, in good

agreement with the predicted value obtained from Rouse-Zimm theory [19].

CONCLUSIONS

The specific instrumentation discussed in this paper represents just two possible realizations of microrheometers for complex fluids. Numerous other designs have been described in the literature. In particular we have not considered particle-tracking techniques or the advent of micro-rheometers based on microfluidic chips. Nonetheless, several common features essential for successful development all microrheometric instruments may be identified:

• In order to obtain *quantitative measurements* (rather than simply qualitative observations of microstructure), it is commonly necessary to perform detailed theoretical or numerical analysis of the system response (e.g. to understand probe-fluid interactions, free-surface effects etc). This need indicates a continuing important role for non-Newtonian fluid dynamics and computational rheology in the future.

• Such dynamical analyses may be simplified and/or rationalized by understanding the relevant dimensionless parameters characterizing the dominant forces and time scales of importance.

• Data acquisition and data analysis frequently requires development or integration of new opto-electronic subsystems and sophisticated image-processing or data reduction algorithms.

As a result of these common features and challenges, the emerging field of microrheometry lies between the capabilities of existing macroscale instrumentation such as bulk rheometers and broadly-accepted microscale hardware such as the atomic force microscope. It will be very interesting to see in the future which group of equipment vendors embraces this middle ground first.

ACKNOWLEDGMENTS: I would like to thank the following students & colleagues, whose research is represented in this paper; Dr. C. Clasen, Dr. J. Bico, N. Kojic, L. Rodd. It is also a great pleasure to acknowledge continuing conversations on the topics of extensional rheology and microrheology with V. Entov, O. Hassager and D. F. James.

REFERENCES

1. E. Meyer, R.M. Overney, K. Dransfeld and T. Gyalog, "*Nanoscience: Friction and Rheology on the Nanometer Scale*", World Scientific, Singapore, (1998) .
2. M. Scherge and S.S. Gorb, "*Biological Micro- and Nano-Tribology*", Springer-Verlag, Berlin, (2001) .
3. D.A. Weitz and D.J. Pine, in "*Dynamic Light Scattering*", (Ed. W. Brown) OUP, Oxford (1992),
4. T.G. Mason, K. Ganesan, J.H. van Zanten, D. Wirtz and S.C. Kuo, *Phys. Rev. Lett* , **79**, 3281, (1997).
5. V. Breedveld and D.J. Pine, *J. Mater. Sci.* , **38**, 4461, (2003).
6. M.J. Solomon and Q. Lu, *Curr. Opin. Colloid & Int. Sci.* , **6**, 430, (2001).
7. F. Scheffold and P. Schurtenberger, *Soft Mater.*, **1**, 139, (2003).
8. A. Mukhopadhyay and S.L. Granick, *Curr. Opin. Coll. & Int. Sci* , **6**, 423, (2001).
9. C. Clasen and McKinley G.H., *J. Non-Newt. Fluid Mech. (Special Issue; Rheometry II Workshop, Wales 2003)* , in press, (2003).
10. F. Vollrath and D. Knight, *Nature*, **410**, 541, (2001).
11. X. Chen, F. Vollrath and D. Knight, *Biomacromol.*, **3**, 644, (2001).
12. R.B Bird, R.C Armstrong and O Hassager, *Dynamics of Polymeric Liquids. Volume 1: Fluid Mechanics*, Wiley Interscience, New York, (1987) .
13. M.W. Denny, *J. Exp. Biol.*, **97**, 337, (1989).
14. M.W. Denny and J.M. Gosline, *J. Exp. Biol.*, **88**, 375, (1980).
15. A.V. Bazilevsky, V.M. Entov and A.N. Rozhkov, in "*Third European Rheology Conference*", (Ed. D.R. Oliver) Elsevier Applied Science, (1990), 41.
16. S.L. Anna and G.H. McKinley, *J. Rheol.*, **45**, 115, (2001).
17. M. Stelter, G. Brenn, A.L. Yarin, R.P. Singh and F. Durst, *J. Rheol.*, **46**, 507, (2002).
18. V.M. Entov and E.J. Hinch, *J. Non-Newt. Fluid Mech.*, **72**, 31, (1997).
19. L.E. Rodd, T.P. Scott, J.J. Cooper-White and G.H. McKinley, *Appl. Rheol.*, submitted, (2004).
20. S.H. Spiegelberg and G.H. McKinley, *J. Non-Newtonian Fluid Mech.*, **67**, 49, (1996).
21. P. Dontula, M. Pasquali, L.E. Scriven and C.W. Macosko, *Rheol. Acta*, **36**, 429, (1997).
22. J. Li and M.A. Fontelos, *Phys. Fluids*, **15**, 922, (2003).